FULL PAPER

Dalton
www.rsc.org/dalton

Solution chemical properties and catecholase-like activity of the copper(II)–Ac-His-His-Gly-His-OH system, a relevant functional model for copper containing oxidases†

A. Jancsó,‡[a] Z. Paksi,[b] N. Jakab,[c] B. Gyurcsik,[b] A. Rockenbauer[d] and T. Gajda*[b]

[a] *Department of Chemistry, University of Turku, FIN-20014 Turku, Finland*

[b] *Department of Inorganic and Analytical Chemistry, University of Szeged, P.O. Box 440, H-6701 Szeged, Hungary. E-mail: tamas.gajda@chem.u-szeged.hu*

[c] *Bioinorganic Chemistry Research Group of the Hungarian Academy of Science, University of Szeged, P.O. Box 440, H-6701 Szeged, Hungary*

[d] *Chemical Research Center, Institute of Chemistry, P.O. Box 17, H-1525 Budapest, Hungary*

Received 31st May 2005, Accepted 26th July 2005
First published as an Advance Article on the web 19th August 2005

The solution chemical properties, superoxide dismutase and catecholase activity of the copper(II)–Ac-His-His-Gly-His-OH (hhgh) complexes were studied to identify functional and structural models of copper-containing oxidases. The solution speciation was determined in the pH range 3–11 by two independent methods (potentiometry and pH-dependent EPR measurements). The results obtained by the two methods agree very well with each other and show the formation of differently protonated CuH_xL complexes (where $x = 2, 1, 0, -1, -2, -3$) in aqueous solution. The spectroscopic (UV–Vis, CD, EPR) data indicate that the coordination of the imidazole rings is a determinant factor in all these complexes. Amide coordinated complexes are dominant only above pH 8. This offers excellent possibilities for structural/functional modelling of copper(II) containing metalloenzymes. Indeed, the $\{3N_{im}\}$ coordinated CuL species (pH = 6–7) has efficient superoxide dismutase-like activity. The $\{3N_{im},OH^-\}$ coordinated $CuH_{-1}L$ possesses outstanding activity to catalyze the oxidation of 3,5-di-*tert*-butylcatechol (H_2dtbc) by dioxygen in 86 wt% methanol–water, providing the first example that copper(II)–peptide complexes are able to mimic copper containing oxidases.

Introduction

The metal-binding properties of His-containing peptides have been extensively studied in order to mimic structural features of metal–protein interaction.[1,2] Although the copper(II)–amide bond appears extremely rarely in metalloproteins, it occurs in the N-terminal copper (and nickel) binding site of some serum albumins. Since albumins are the major transporters of copper(II) in blood, a great number of model studies, using oligopeptides with histidine at the third position, have been undertaken.[3–6] The discovery of the high-affinity copper binding sites of prion[7,8] and β-amyloid[9] proteins, and the possibility of their involvement in the pathogenesis of the corresponding prion[10] and Alzheimer's[11] diseases, gave a new stimulus to the coordination chemistry of His-containing peptides.[12,13] Nevertheless, it has been recognized for a long time, that the high ability of copper(II) ion to deprotonate amide nitrogens strongly restricts the analogy between copper(II) complexes of small peptides and copper containing metalloenzymes. On the other hand, the coordination mode of His-containing peptides strongly depends on the number and position of the His residue(s) in the peptide and those of the nearby donor groups.[1,2] Therefore, using an appropriate peptide sequence the amide-coordination might be prevented in the neutral pH range.

In view of enzyme modelling, there is a substantial interest in copper(II)–peptide complexes with exclusive imidazole coordination at neutral pH. Several type II copper proteins are known to bind to the central copper(II) ion only by histidine imidazole nitrogens, *e.g.* Cu–Zn superoxide dismutase, amine oxidases or nitrite reductases. The recently determined crystal structure of quercetin 2,3-dioxygenase from *Aspergillus japonicus* indicated[14] two distinct geometries in the active centre, a distorted tetrahedral $\{3N_{im},H_2O\}$ (70%), and a distorted trigonal bipyramidal $\{3N_{im},COO^-,H_2O\}$ (30%) type coordination. Only peptides with three or more histidine residues may provide a real possibility to coordinate the metal ions solely by the side chain donor groups in the physiological pH range. This was confirmed in a few cases by some peptide complexes of nickel(II)[15–17] and copper(II),[18] containing more than two His units.

The dismutation of superoxide and the oxidation of 3,5-di-*tert*-butylcatechol (H_2dtbc) are probably the two most widely used test reactions to screen the redox properties of biomimetic catalysts. Although a great number of model complexes have been shown to act as efficient superoxide dismutase[19–24] or catecholase-like[25–30] catalysts, to our knowledge, no reports are available on the catecholase activity of copper(II)–peptide complexes.

As a continuation of our work on the coordination chemistry of imidazole ring,[31–34] here we present solution equilibrium and structural investigations of the zinc(II)– and copper(II)–Ac-His-His-Gly-His-OH (hhgh) system, as a structural model of zinc and copper proteins. In order to test the redox activity of the formed copper(II) complexes, we have also studied their superoxide dismutase and catecholase activity.

During our experimental work, a solution equilibrium study of the copper(II)–hhgh system has been published by Sóvágó *et al.*[35] Although the present report suggests similar speciation, our spectroscopic data, especially those obtained from the pH-dependent EPR study, together with the kinetic investigations, considerably extend the knowledge on this system.

† Electronic supplementary information (ESI) available: Inhibition of the Nitroblue Tetrazolium (NBT) reduction as a function of the copper(II) concentration in 0.05 M phosphate buffer and the inhibition caused by Cu,Zn-SOD (Fig. S1), the CD spectra of the copper(II)–hhgh system at different pH in 86 wt% methanol–water solvent mixture (Fig. S2) and the pH dependence of the average CD intensity between 355 and 365 nm. See http://dx.doi.org/10.1039/b507655b

‡ Present address: Department of Inorganic and Analytical Chemistry, University of Szeged, P. O. Box 440, H-6701 Szeged, Hungary.

DOI: 10.1039/b507655b

Table 1 Formation constants and derived data of the zinc(II)– and copper(II)–hhgh complexes (the estimated errors in the last digit are in parentheses, $I = 0.1$ M NaCl, $T = 298$ K). The pK values of hhgh are as follows: p$K_1 = 2.52(2)$, p$K_2 = 5.95(1)$, p$K_3 = 6{,}61(1)$, p$K_4 = 7.73(1)$

logβ_{pqr}	Zn^{II}[a]	Cu^{II}[a]	Cu^{II}[b]	pK_{pqr}[c]	Cu^{II}[a,d]	Cu^{II}[a,e]
logβ_{121}	—	18.50(4)	—	pK_{121}	4.31	4.39
logβ_{111}	11.47(2)	14.19(1)	14.11(5)	pK_{111}	5.81	5.26
logβ_{101}	5.10(3)	8.38(2)	8.48(5)	pK_{101}	7.01	6.93
logβ_{1-11}	−1.51(3)	1.37(2)	1.29(5)	pK_{1-11}	8.10	8.38
logβ_{1-21}	—	−6.73(2)	−6.67(5)[f]	pK_{1-21}	9.93	9.86
logβ_{1-31}	—	−16.66(2)	−16.64(5)			
F.P.[g]	0.0007	0.0011				
N.P.[h]	498	635				

[a] Derived from potentiometric data; [b] Derived from EPR data; [c] $pK_{pqr} = \log\beta_{pqr} - \log\beta_{p(q-1)r}$; [d] This work; [e] Ref. 35; [f] The individual logβ values are −6.93(5) and −7.02(5) for $CuH_{-2}L$(a) and $CuH_{-2}L$(b), respectively; [g] Fitting parameter (cm^3); [h] Number of the experimental points.

Results and discussion

The potentiometric titration curves of the ligand can be described considering four protonation processes (Table 1). The values of pK_1, pK_2 and pK_3 are in the range generally observed for His-containing peptides, however, pK_4 (= 7.73) is *ca.* 0.6–1.4 units higher than in case of the related systems.[5,6,9,13,17] This indicates relatively strong H-bonding network within the monoprotonated ligand molecule.

Zinc(II) complexes

The three complexes detected in the Zn^{II}–hhgh system (ZnHL, ZnL, $ZnH_{-1}L$) are minor species with respect to the free zinc(II) up to pH 7, where precipitation occurred, even in case of ligand excess. The log$K$ value for the reaction Zn^{2+} + HL = ZnHL (log$K$ = 3.74) is somewhat higher than the corresponding log$\beta_{101} = 3.29$ reported for the Zn^{II}–Ac-His-Pro-His-NH_2 system,[36] suggesting that the carboxylate group may also coordinate in this species beside the two imidazole nitrogens. In the complex ZnL probably all three imidazole rings are coordinated to the metal ion (log$\beta_{101} = 5.10(3)$, pK_{ZnHL}(= 6.37) < pK_4(= 7.73)). Although, the $\{3N_{im}\}$ type coordination is one of the favored binding mode of zinc(II) in biological systems, it is not able to keep the metal ion in the solution in the present case.

Copper(II) complexes

The comparative evaluation of the potentiometric, UV-Vis and CD spectroscopic data indicated the formation of six differently protonated species above pH 3 (Fig. 1, Table 1). The pH dependent EPR titration confirmed this observation, but reflected the presence of binding isomers in case of the complex $CuH_{-2}L$ (see also the Experimental part). Taking into consideration seven complex species beside the aqua ion, the experimental data obtained by the four different methods can be described satisfactorily. The two independent sets of formation constants, derived from our potentiometric and EPR data, are in good agreement (Table 1), but are somewhat different from those reported recently.[35] On the other hand, the speciation and

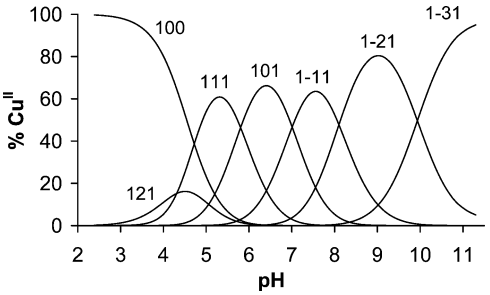

Fig. 1 Speciation diagram of the copper(II)–hhgh system ([Cu^{II}] = [hhgh] = 0.001 M, $T = 298$ K, $I = 0.1$ M NaCl, the species are denoted by their *pqr* numbers).

thus the stepwise deprotonation constants of the complexes are rather similar (see the pK_{pqr} values in Table 1), indicating that the deviation of formation constants originate from the differences of the pK values used.

The complex CuH_2L is only a minor species in the acidic region, thus its spectral parameters could not be determined. The monoprotonated CuHL is dominant in the solution around pH 5. Since p$K_{121} \ll$ pK_3 (Table 1), both neutral imidazole rings are probably coordinated in CuHL. Indeed, the equilibrium constant for the reaction Cu^{2+} + HL = CuHL (log$K$ = 6.46) agrees well with that of a related $\{2N_{im}\}$ coordinated complex.[22] The spectral parameters of CuHL (Table 2) are also in agreement with the equatorial coordination of two imidazole nitrogens.[36,37]

Around pH 6.5, the complex CuL dominates in the solution. The difference between pK_{111} (5.81) and pK_4 (7.73) as well as the decrease in both g_0 and $\lambda^{d-d}{}_{max}$ indicates the coordination of all the three imidazole rings in CuL. Its formation constant (logβ_{101} = 8.38) is similar to those of the related $\{3N_{im}\}$ coordinated species.[9,17] The CD spectrum of CuL (Fig. 2B) has low intensity bands both in the charge-transfer (CT) and d-d regions, further supporting the coordination of only imidazole nitrogens. On the other hand, the d–d maximum ($\lambda^{d-d}_{max} = 650$ nm) shows a notable red shift as compared to the analogous $\{3N_{im}\}$ complexes (ref. 9 607 nm and ref. 17 587 nm). In addition,

Table 2 EPR and UV-Vis spectroscopic parameters of the various complexes formed in the copper(II)–hhgh system[a] (the estimated errors[b] for the g_0, A_0, A_N values and relaxation parameters are ±0.0005, ±0.8 G, ±1.0 G and ±1.0 G, respectively)

Species	λ^{d-d}/nm	g_0	A_0/G	A_{N0}/G	a/G	β/G	γ/G
Cu^{2+}		2.1927	35.1	—	57.0	−2.4	0.2
CuHL	680	2.1546	58.4	12.3 13.2	58.4	−32.7	7.9
CuL	650	2.1250[c]	58.1[c]	15.9[c] 39.2[c]	52.4[c]	−37.6[c]	15.4[c]
$CuH_{-1}L$	596	2.1126	74.3	3 × 10.0	72.2	−33.2	12.5
$CuH_{-2}L$(a)	580[d]	2.1055	69.0	2 × 11.3 2 × 13.4	30.0	−23.5	6.7
$CuH_{-2}L$(b)	580[d]	2.0815	57.5	4 × 16.1	24.4	−4.3	3.3
$CuH_{-3}L$	547	2.0845	84.2	10.0 3 × 13.6	38.1	−21.8	5.8

[a] The hyperfine coupling constants and the relaxation parameters refer to the isotope ^{63}Cu; [b] In case of intense electron relaxation (*e.g.* CuHL, $CuH_{-1}L$) the A_{N0} values have higher uncertainties; [c] Formal parameters, see the text; [d] Average value of the two isomers.

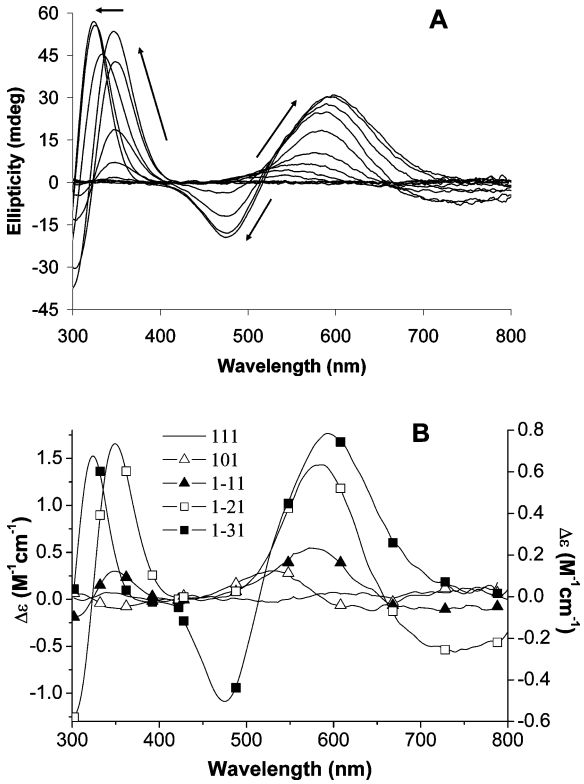

Fig. 2 pH Dependence of the CD spectra (A) of the copper(II)–hhgh system ([Cu^{II}] = [hhgh] = 0.6 mM, T = 298 K, I = 0.1 M NaCl, pH = 2.61–11.96), and the calculated individual spectra of the formed species (B).

the EPR spectrum of this species can only be simulated by an anomalously high super-hyperfine (shf) coupling constant (Table 2, Fig. S2, see ESI†). It should be noted that the EPR parameters of the complex CuL, listed in Table 2, provide only a formal description of the component curve. It is probably the superposition of two or more individual spectra. The spectral pattern and the 39 G shf coupling constant may indicate the presence of a dimer species with spin-exchange interaction between the metal centres. However, our attempt to simulate the spectral data considering a dimer species (Cu_2L_2) or a monomer–dimer equilibrium (CuL and Cu_2L_2) failed. Tentatively we propose that beside the monomer CuL an imidazole bridged $(CuL)_n$ cluster(s) may also form, which hinders the correct deconvolution of the spectra due to its intense electron relaxation.

The next process ($CuL = CuH_{-1}L + H^+$, $pK_{101} = 7.01$) can be attributed to the deprotonation of (i) an amide nitrogen, or (ii) a coordinated water molecule. The d–d transition and the EPR spectrum of the species $CuH_{-1}L$ ($\lambda_{max}^{d-d} = 596$ nm, $g_0 = 2.1126$, $A_0 = 74.3$ G) may correspond to either a $\{3N_{im},OH^-\}$ or a $\{2N_{im},N^-,H_2O\}$ type coordination. On the other hand, the low intensity of d–d and CT bands on the CD spectrum of this species (Fig. 2B) does not support the presence of coordinated amide nitrogen in $CuH_{-1}L$. One has to mention, that the coordination of the Gly(3) amide nitrogen would not cause strong chiral perturbation on the metal ion. However, peptides with HXH sequence undergo two strongly overlapping amide deprotonations in the presence of copper(II) ($\Delta pK = pK_{1-11} - pK_{101} =$ 0.19 (Ac-HLHWH-NH_2),[17] 0.18 (Ac-HGH-OH),[35] −0.04 (Ac-ETHLHWHTVAKET-NH_2),[9] −0.63 (Ac-HGH-NHMe),[35] and $\Delta pK < -1$ for Ac-HVH-NH_2[22] or HGHG[38]), due to the preferred formation of a $\{N_{im}/NH_2,N^-,N^-,N_{im}\}$ coordinated species. In the copper(II)–hhgh system $\Delta pK = 1.09$ (ref. 35 1.46), *i.e.* strongly cooperative deprotonations were not observed. Although none of the two possible coordination modes ($\{3N_{im},OH^-\}$ or $\{2N_{im},N^-,H_2O\}$) can be definitely excluded, our data, including the results of the kinetic experiments, suggest the deprotonation of a coordinated water molecule (Scheme 1).

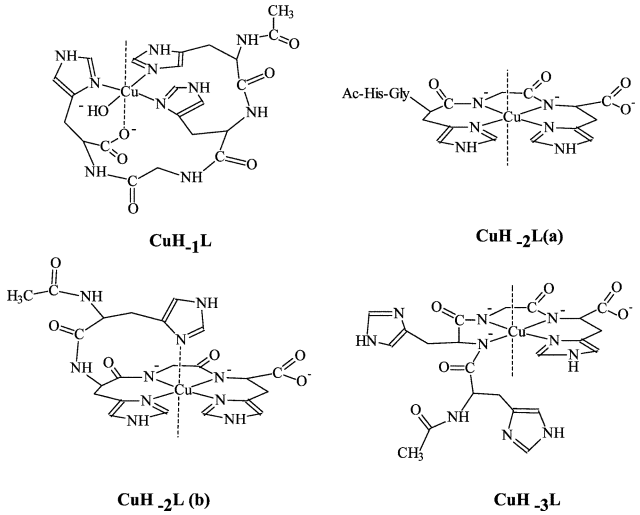

Scheme 1 Suggested structures for the major complexes (note that for $CuH_{-1}L$ the amide coordination cannot be definitely ruled out). The open coordination sites are occupied by water molecule(s).

The formation of the $CuH_{-2}L$ species ($CuH_{-1}L = CuH_{-2}L + H^+$, $pK = 8.10$) results in fundamental changes of the CD and EPR spectra (Fig. 2 and 3). The intensity of the CD bands increase both in the CT and d–d region (Fig. 2). This reflects a rather strong chiral perturbation mediated by the

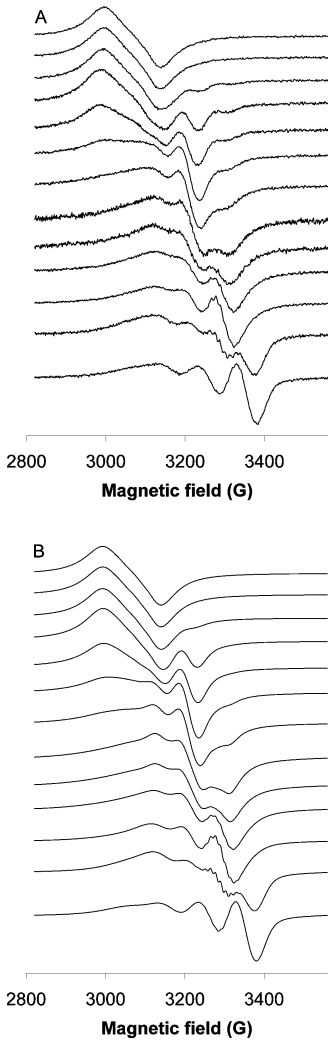

Fig. 3 pH Dependence of the experimental (A) and calculated (B) EPR spectra of the copper(II)–hhgh system ([Cu^{II}] = [hhgh] = 1.3 or 0.6 mM, T = 298 K, I = 0.1 M NaCl, pH = 2.3–10.8). The calculated spectra of the individual species are presented in Fig. S2 in ESI†.

metal coordination of amide nitrogen(s). The evaluation of the pH-dependent EPR spectra indicated the presence of two binding isomers with the composition of $CuH_{-2}L$ (see also the Experimental part). The well resolved shf pattern on the spectrum of the (a) isomer, as well as its g_0 value indicates the coordination of four nitrogens in the equatorial plane of copper(II). Considering its composition, a $\{2N_{im},2N^-\}$ type coordination, with the participation of Gly(3) and His(4) amide nitrogens, can be proposed for $CuH_{-2}L$(a). This structure is identical to that suggested earlier for the species $CuH_{-2}L$.[35] However, our EPR data indicate the presence of a (b) isomer, too, having considerably lower A_0 and g_0 values. Since the decrease of g_0 generally goes together with the increase of A_0, the above observation indicates some distortion, probably caused by an axially coordinated nitrogen in $CuH_{-2}L$(b). The imidazole ring of His(1) may, indeed, coordinate in the axial position (Scheme 1), resulting in a somewhat higher stability for the (b) isomer. The position of the d–d band determined for the complex $CuH_{-2}L$ (Fig. S1.B,† $\lambda_{max}^{d-d} = 580$ nm), shows an important red shift as compared to that of the related $\{N_{im},N^-,N^-,N_{im}\}$ coordinated $CuH_{-2}L$ complex of Ac-HVH-NH_2 and HGHG ($\lambda_{max}^{d-d} = 530$ nm).[22,38] Although, the spectrum depicted in Fig. S1.B† is a superposition of those of the two isomers, the fairly important red shift confirms the axial imidazole coordination at least in one of them. The $\{N_{im},N^-,N^-,N_{im} + N_{im}\}$ coordinated $CuH_{-2}L$(b) has analogous structure to that suggested for the high affinity copper binding site of amyloide precursor protein.[9,17]

Above pH 9 a new deprotonation ($CuH_{-2}L = CuH_{-3}L + H^+$, $pK = 9.93$) was observed, which was attributed to the metal promoted deprotonation of a third amide nitrogen. The increased negative chiral contribution of the amide nitrogens (Fig. 2.B) on the CD spectrum of $CuH_{-3}L$, and its spectral parameters ($\lambda_{max}^{d-d} \sim 547$ nm, $g_0 = 2.0844$, $A_0 = 84.2$ G) indicate, indeed, a further rearrangement of the coordination sphere, *i.e.* the imidazole ring of His(2) is replaced by the deprotonated amide nitrogen of the same unit in the equatorial plane of copper(II). Sóvágó *et al.* suggested the axial coordination of the His(2) imidazole ring in this species.[35] The analogous $\{N^-,N^-,N^-,N_{im}\}$ coordinated Cu^{II} complex of Ac-HVH-NH_2 ($\lambda_{max}^{d-d} = 530$ nm)[22] has a somewhat different d–d spectrum. Although this deviation may indicate an axial imidazole coordination, the fairly high A_0 value does not support strong axial binding. Therefore, we suggest $\{N^-,N^-,N^-,N_{im}\}$ type coordination in $CuH_{-3}L$ (Scheme 1), with the C-terminal imidazole ring in the equatorial plane of copper(II). Since further deprotonation was not observed up to pH 11.2, and the CD spectra detected at pH 11.0 and 11.96 are almost identical (Fig. 2), our data do not support the formation of $CuH_{-4}L$, reported earlier.[35]

A remarkable property of the Cu^{II}–hhgh system is that in the neutral pH range the peptide is coordinated to the metal ion solely by its side chain imidazole nitrogens (in CuL formed between pH 6–7). This is a rarely observed feature for the copper(II)–peptide complexes,[18,35] which may provide a possibility to mimic redox active copper containing enzymes. Indeed, the CuL complex of hhgh shows notable similarities to the active centrum of quercetin 2,3-dioxygenase, concerning even the carboxylate group near the metal ion.[14] Therefore, we performed kinetic studies to check the redox activity of this system. Although, a number of copper(II)–peptide complexes[19–24] have been shown to possess superoxide dismutase-like activity, their ability to mimic copper(II) containing oxidases has not been reported so far.

Superoxide dismutase activity

The SOD-like activity of the copper(II)–hhgh system was tested indirectly, by its ability to inhibit the reaction between the O_2^- radical and NBT. For comparison, the activity of the native Cu,Zn-SOD from bovine erythrocytes was also investigated. The determined IC_{50} values are listed in Table 3, together with those of some highly active SOD mimics, taken from the literature. Although the activity of the copper(II)–hhgh complexes is *ca.* thirtyfold lower than that of the native enzyme, it is one of the most active model systems reported so far. It is noteworthy, that at pH = 6.8 almost complete (97.2%) inhibition was achieved using 0.5 μM total concentration of copper(II) (see Fig. S3 in ESI†). The correct interpretation of the observed SOD-like activity requires a knowledge of the speciation in the very dilute solutions used ($[Cu^{2+}] \leq 1$ μM), which may be considerably different from that depicted in Fig. 1. Indeed, at low concentrations considerable amounts of free copper(II) is present in the equimolar solution, whilst there is practically no free metal ion when tenfold excess of the ligand is used (see the actual speciation in the legend of Fig. S3†). The IC_{50} values listed in Table 3 confirm that the SOD-like activity is mostly related to the copper(II)–peptide complexes, and indicate somewhat higher SOD-like activity for the species CuL, in agreement with its lower equatorial field strength,[22] and higher accessibility for the O_2^- radical ligand.

Table 3 IC_{50} (μM) values of the Cu^{II}–hhgh complexes, the native Cu,Zn-SOD enzyme and some of the most active model compounds reported so far[a]

Complex	IC_{50} (μM)	Ref.
Cu^{II}–hhgh; 1/1 (pH 6.8)	0.13	This work
Cu^{II}–hhgh; 1/1 (pH 7.5)	0.15	This work
Cu^{II}–hhgh; 1/10 (pH 7.5)	0.25	This work
Cu,Zn-SOD (pH 6.8)	0.0045	This work
$[CuL^1]$ (pH 7.4)	0.09	19
Cu–(cyclo-His-His)	0.11	20
$[CuL^2{}_2(py)_2]$; (pH 7.8)	0.146	21
Cu^{II}–Ac-HVH-NH_2; 1/1 (pH 7.4)	0.20	22
Cu^{II}–L^3; 1/1000 (pH 7.4)	0.24	23
$[CuZnL^4]$	0.24	24
Cu^{II}–carnosine; 1/1000 (pH 7.4)	0.80	23
$Cu(HPO_4)$ (pH 7.4)	1.06	23

[a] L^1 = *N*,*N*′-bis(2-acetylpyrazyl)methylene-1,3-diaminopropane, L^2 = *N*-2-(4-methylbenzothiazole)benzenesulfonamidate, L^3 = 6-deoxy-6-(β-alanylhistidyl)-β-cyclodextrin, L^4 = 4,5-bis(di(2-pyridylmethyl)-aminomethyl)imidazolate

Oxidation of 3,5-di-*tert*-butylcatechol (H_2dtbc)

The catalytic oxidation of H_2dtbc has been widely studied to screen the catecholase activity of various copper(II) complexes.[25–30] Since catechol oxidases are type 3 copper enzymes,[39] mostly dinuclear complexes were used for the biomimetic studies. Nevertheless, several mononuclear complexes have been reported to possess important catecholase activity.[25,29]

In order to check the ability of the copper(II)–hhgh system to catalyse redox reactions, we followed the oxidation of H_2dtbc to 3,5-di-*tert*-butyl-1,2-benzoquinone (dtbq) by dioxygen in the presence and absence of the copper(II)–hhgh complexes in 86 wt% methanol–water solvent saturated with O_2. Initially, the $\{3N_{im}\}$ coordinated CuL complex was expected to possess oxidase activity, since it mimics the active centre of several type 2 copper enzymes, but in the neutral pH range practically no activity was observed (Fig. 4). Above pH 8, however, important catalytic activity developed, which levels off around pH 10. The increasing H_2dtbc concentration at pH 10.18 results in saturation kinetics above fortyfold excess of the substrate (Fig. 5). These experimental data can be well fitted supposing a deprotonation process ($pK \sim 8.7$) leading to the catalytically active species and applying the Michaelis–Menten approach. In order to verify this hypothesis, we studied the complex formation processes under the conditions used for the kinetic measurements (86 wt% methanol–water, $[Cu^{2+}] = [hhgh] = 5.5 \times 10^{-5}$ M). Due to the rather low concentrations, only the CD spectroscopic study provided valuable information (see Fig. S4

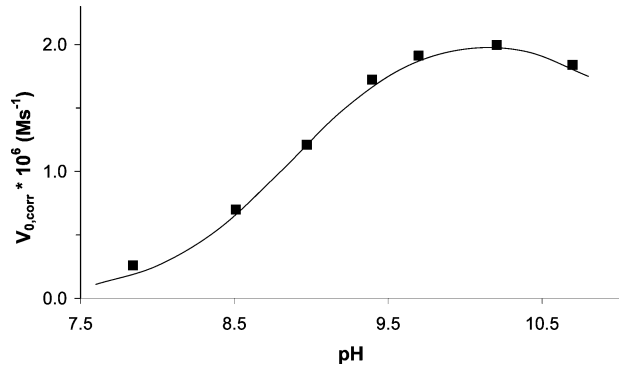

Fig. 4 Dependence of the initial reaction rate on pH for the oxidation of H_2dtbc promoted by the copper(II)–hhgh system (86 wt% methanol–H_2O, $[Cu^{II}] = [hhgh] = 0.0555$ mM, $[H_2dtbc] = 2.488$ mM, $T = 298$ K). The solid line was calculated by the simultaneous evaluation of the data depicted in Fig. 5 and 6, using eqn (1).

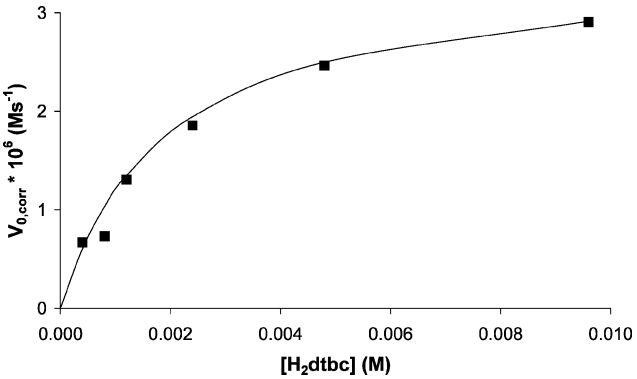

Fig. 5 Dependence of the initial reaction rate on the H_2dtbc concentration for the oxidation promoted by the copper(II)–hhgh system (86 wt% methanol–H_2O, $[Cu^{II}] = [hhgh] = 0.0555$ mM, pH = 10.18, $T = 298$ K). The solid line was calculated by the simultaneous evaluation of the data depicted in Fig. 5 and 6, using eqn (1).

and S5 in the ESI†). Between pH 7–8 the complex $CuH_{-1}L$ is the sole species in the solution (as expected, the neutral species is more stable in 86 wt% methanol–water than in pure aqueous solution). The two successive deprotonations of this species can be described by $pK_1 = (9.6 \pm 0.1)$ and $pK_2 = (11.0 \pm 0.2)$ (see Fig. S5†), thus the formation of $CuH_{-2}L$ and $CuH_{-3}L$ shifted considerably to the alkaline region as compared to the analogous processes in pure aqueous solution. Consequently, the above mentioned hypothesis cannot be valid, since in the absence of H_2dtbc no deprotonation occurs with $pK \sim 8.7$ in 86 wt% methanol–water solution. Instead, the reaction pathways depicted in Scheme 2 can explain the observed kinetic data. The oxidation of H_2dtbc is related to the mixed ligand complex CuL(dtbc), since the coordination of catecholate dianion is a necessary step of the copper(II) catalyzed oxidation. This mixed ligand complex forms in a pH-dependent step around pH 8–10. In a nearly parallel reaction the formation of $CuH_{-2}L$ takes place. At pH 10, the complexes CuL(dtbc) and $CuH_{-2}L$ are the major species in the solution. In fact, the increasing initial rate with increasing substrate concentration (Fig. 5) is the consequence of the shift of the equilibrium between $CuH_{-2}L$ and CuL(dtbc), in favour of the latter species. Above pH 10, the formation of $CuH_{-3}L$ results in a decreasing concentration of the mixed ligand complex CuL(dtbc), and thus decreasing initial rate of the oxidation.

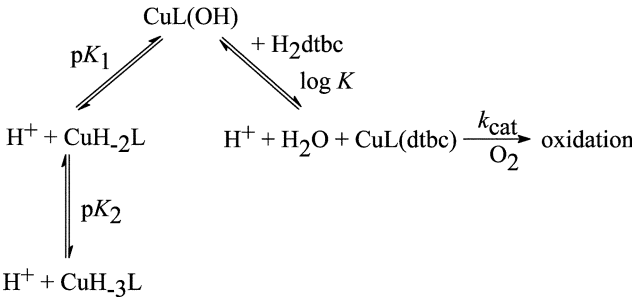

Scheme 2 Suggested reaction pathway in 86 wt% methanol–H_2O solvent.

The pH dependent oxidation of H_2dtbc by copper(II) complexes has already been reported by Neves *et al.*[28,30] The mechanism suggested by these authors involved the deprotonation of two metal-bound water molecules, which is followed by the coordination of H_2dtbc to the dinuclear complex in a pH independent process. However, the catechol derivatives have a strong coordination ability, especially above pH 7. Their presence as a second ligand may have a fundamental influence on the speciation detected in the binary (copper(II)–ligand) systems. Considering the observations collected in the numerous copper(II)–ligand–catechol ternary systems,[40,41] the pH dependent formation of the catecholate containing ternary complex(es) is a very general phenomenon, indeed. However, in such cases the classical form of the Michaelis–Menten equation is not applicable. In our system the reaction rate corrected by the autooxidation can be expressed by the following equation (see Scheme 2):

$$\begin{aligned} V_{corr} &= k_{cat}[CuL(dtbc)] \\ &= k_{cat} \times \frac{[Cu]_{tot}}{\frac{[H^+]}{K[H_2dtbc]} + 1 + \frac{K_1}{K[H_2dtbc]} + \frac{K_1K_2}{K[H_2dtbc][H^+]}} \\ &= \frac{k_{cat}K\,[Cu]_{tot}\,[H_2dtbc][H^+]}{[H^+]^2 + K[H_2dtbc][H^+] + K_1[H^+] + K_1K_2} \end{aligned} \quad (1)$$

where $[Cu]_{tot}$ is the analytical concentration of copper(II).

The simultaneous evaluation of the data depicted in Fig. 4 and 5, using eqn (1), resulted in the following constants (Scheme 2): $k_{cat} = (0.063 \pm 0.007)$ s^{-1}, $\log K = (-6.5 \pm 0.1)$, $pK_1 = (9.3 \pm 0.1)$ and $pK_2 = (11.0 \pm 0.3)$. The values of pK_1 and pK_2 calculated from the CD measurements and from the kinetic data (both in 86 wt% methanol–water) agreed well with each other. Log$K$ is in the expected range, since a similar value ($\log K = -5.16$) was reported[41] for an analogous reaction ($CuH_{-1}A + H_2B = CuAB + H^+$, where A = Gly-Gly and H_2B = catechol) in aqueous solution. The value of k_{cat} indicates outstanding catecholase activity of the copper(II)–hhgh system, it corresponds to the turnover rate of 227 h^{-1}.

The time course of the reaction catalyzed by the complex $CuH_{-1}L$ is shown in Fig. 6. Under the conditions used, the initial concentration of CuL(dtbc) is only 2.2×10^{-6} M, but the reaction is 90% complete in 55 min. In fact, two reactions run parallel in the solution: the catalyzed reaction and the autooxidation. The latter represents only a few % of the overall process (at pH = 8.58 the rate constant of the autooxidation (k_{auto}) is $(3.0 \pm 0.5) \times 10^{-5}$ s^{-1}). Considering both reactions, the reaction rate can be expressed as

$$\begin{aligned} \frac{d[S]}{dt} &= -k_{auto}[S] - k_{cat}[CuL(dtbc)] \\ &= -k_{auto}[S] - k_{cat} \times \frac{A[S]}{B + C[S]} \end{aligned} \quad (2)$$

where $[S] = [H_2dtbc]$, $A = [Cu]_{tot}K[H^+]$, $B = [H^+]^2 + K_1[H^+] + K_1K_2$ and $C = K[H^+]$ (see eqn (1) for the expression of

[CuL(dtbc)]). The integration of eqn (2) results in

$$t = \frac{B(\ln [S]_0 - \ln[S]) + k_{cat}AC\left\{\ln(k_0B + k_{cat}A + k_0[S]_0) - \ln(k_0B + k_{cat}A + k_0[S])\right\}}{k_0B + k_{cat}A} \quad (3)$$

From the data shown in Fig. 6, $k_{cat} = (0.09 \pm 0.01)$ s^{-1} can be calculated using eqn (3) and keeping all other parameters constant. The two values of k_{cat} (0.063 ± 0.007 s^{-1} obtained from Figs. 4, 5 and 0.09 ± 0.01 s^{-1} from Fig. 6) agree well with each other, considering the uncertainties of the parameters k_0, K, K_1 and K_2, as well as the different experimental procedures (initial slope and integral method, respectively).

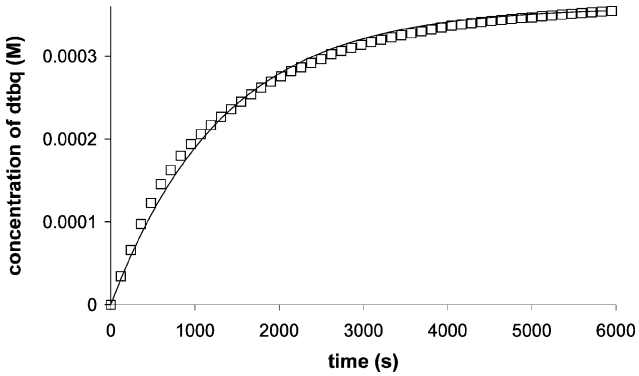

Fig. 6 The oxidation of H_2dtbc catalyzed by the complex $CuLH_{-1}$ (pH = 8.58, $[H_2dtbc]_{ini} = 0.36$ mM, $[Cu^{II}]_{tot} = [hhgh]_{tot} = 0.0555$ mM in 86 wt% methanol–water solution saturated with O_2; the initial concentration of CuL(dtbc) under these conditions is 0.0022 mM; the autooxidation of H_2dtbc at this pH represents only ~3% of the overall effect). The solid line was calculated using eqn (3).

Based on the solution spectroscopic studies, the complex $CuH_{-1}L$ may possess either $\{3N_{im},OH^-\}$ or $\{2N_{im},N^-,H_2O\}$ type coordination in its equatorial plane. The reduction of copper(II) to copper(I) is generally not favored when a strong equatorial field (*i.e.* coordinated amide nitrogen(s)) is present around the metal ion, since it stabilizes the +2 oxidation state. Bearing this in mind, the high catecholase activity of $CuH_{-1}L$ would suggest $\{3N_{im},OH^-\}$ type coordination. The possibility of the involvement of the metal-bound hydroxide ion in a proton-transfer process which promotes the metal coordination of H_2dtbc, may further support the $\{3N_{im},OH^-\}$ binding mode in $CuH_{-1}L$.

A further point to be clarified is the two-electron oxidation of H_2dtbc, which cannot be promoted by a single mononuclear copper(II) complex. A recent mechanistic study on the $[Cu(idpa)]^{2+}$ catalyzed oxidation of H_2dtbc by Speier *et al.*[29] (idpa = 3,3′-iminobis(*N*,*N*-dimethylpropylamine) indicated the formation of a mononuclear Cu^{I}(idpa)(dbsq) complex (dbsq = di-*tert*-butylsemiquinone radical) which reacts with dioxygen leading to a peroxo-bridged Cu^{II} dimer, then dtbq and H_2dtbc are formed by disproportionation. A similar mechanism may operate in our case, too. Although the above indicates that a rather complicated mechanism may operate during the catalytic cycle, the results show the simple model depicted in Scheme 2, and the inherent assumption that the rate determining step is the formation of CuL(dtbc), to be sufficient for a kinetic description.

Conclusion

The potentiometric and pH-dependent spectroscopic data obtained in the copper(II)–hhgh system indicated the formation of differently protonated CuH_xL complexes ($x = 2, 1, 0, -1, -2, -3$). In the neutral pH range the ligand is coordinated to the metal ion by its imidazole nitrogens, the amide coordinated complexes dominate only above pH 8. The pH-dependent EPR data reflected the presence of two binding isomers in the case of $CuH_{-2}L$ with $\{N_{im},N^-,N^-,N_{im} + N_{im}\}$ and $\{N_{im},N^-,N^-,N_{im}\}$ coordination modes. The metal binding of three side-chain imidazole rings in CuL and $CuH_{-1}L$ shows notable similarities to the active centrum of several copper-containing enzymes. Therefore, we performed kinetic studies to establish the redox activity of this system. Although the complex CuL shows high superoxide dismutase activity, it does not promote the oxidation of H_2dtbc by dioxygen. This reaction is, however, very efficiently catalyzed by the $CuH_{-1}L$ species, providing the first example that copper(II)–peptide complexes are able to mimic copper-containing oxidases.

Experimental

Materials

Copper(II) and zinc(II) chloride (Fluka) solutions were standardized complexometrically. pH-metric Titrations were performed by NaOH (Fluka) standard solution. Ac-His-His-Gly-His-OH (Bachem), xanthine, xanthine oxidase, Nitroblue Tetrazolium, Cu,Zn-SOD and 3,5-di-*tert*-butylcatechol (Sigma) were used without further purification (some samples of Ac-His-His-Gly-His-OH contained unknown potentiometrically active impurities other than acetate ion, therefore these samples were not used in our studies).

pH-metric Measurements

The protonation and coordination equilibria were investigated by potentiometric titration in aqueous solution ($I = 0.1$ M NaCl, and $T = 298.0 \pm 0.1$ K) under an argon atmosphere, using an automatic titration set including a PC controlled Dosimat 665 (Metrohm) autoburette and an Orion 710A precision digital pH-meter. The Orion 8103BN semimicro pH glass electrode was calibrated[42] *via* the modified Nernst equation:

$$E = E_0 + K\log[H^+] + J_H[H^+] + \frac{J_{OH}K_w}{[H^+]}$$

where J_H and J_{OH} are fitting parameters in acidic and alkaline media for the correction of experimental errors, mainly due to the liquid junction and to the alkaline and acidic errors of the glass electrode; $K_w = 10^{-13.75}$ M^2 is the autoprotolysis constant of water.[43] The parameters were calculated by the non-linear least squares method. The complex formation was characterized by the following general equilibrium process:

$$pM + qH + rL \rightleftharpoons^{\beta_{M_pH_qL_r}} M_pH_qL_r$$

$$\beta_{M_pH_qL_r} = \frac{[M_pH_qL_r]}{[M]^p[H]^q[L]^r}$$

where M denotes the metal ion and L the non-protonated ligand molecule. Charges are omitted for simplicity, but can be easily calculated taking into account the composition of the fully protonated peptide (H_4L^{3+}). The corresponding formation constants ($\beta_{M_pH_qL_r} \equiv \beta_{pqr}$) were calculated using the PSEQUAD computer program.[44]

The protonation constants were determined from 4 independent titrations (50–60 data points per titration). The ligand was obtained as an acetate salt. The concentration of its stock solution was determined by potentiometric titrations using pK = 4.57 for the acetic acid. The complex formation constants were

evaluated from 8 independent titrations (60–80 data points per titration). The metal-to-ligand ratios were 1 : 1 and 1 : 2, with the ligand concentrations between 4.0×10^{-4} and 1.3×10^{-3} M. The formation constants of the copper(II) and zinc(II) acetate complexes ($\log K = 1.8$ and 0.86, respectively) were taken into account.

Electronic absorption and CD measurements

UV-VIS spectra were measured on a Hewlett Packard 8452A diode array spectrophotometer. The CD spectra were recorded on a Jasco J-710 spectropolarimeter in the wavelength interval from 300 to 800 nm. The metal ion concentration was 6×10^{-4} M in a cell with 1 cm optical pathlength. The individual spectra of the copper(II) complexes were calculated by the previously mentioned computer program PSEQUAD.

EPR measurements

The EPR titrations were performed in 12 cm^3 solution under an argon atmosphere. The initial concentration of hhgh was 1.3×10^{-3} M (6.0×10^{-4} M for the spectra measured in the neutral pH range). A Masterflex CL peristaltic pump ensured the circulation (14 cm^3 min^{-1}) of the solution through the capillary tube in the cavity. The EPR spectra were taken after equilibration/circulation for 3 min at a chosen pH at room temperature ($T = 298$ K) on an upgraded JEOL-JES-FE3X spectrometer with 100 kHz field modulation, using a manganese(II)-doped magnesium oxide powder for the calibration of the magnetic field. The series of EPR spectra were evaluated by a recently developed two dimensional simulation method able to adjust the formation constants of the various species together with the magnetic parameters of the component EPR spectra.[45] Between pH 8–10, where the $CuH_{-2}L$ species has the largest concentration, the fit of the EPR spectra was not satisfactory. This indicated that additional species have to be taken into account. Since complexes with further compositions were supported by neither the pH-metric nor the EPR data, structural isomers were considered in the calculation for the complex $CuH_{-2}L$. In order to justify the necessity of new species, the improvement of the fit was analysed. We used a criterion of normalized regression parameter R_n defined as

$$1 - R_n = N(1 - R)$$

which indicates wether the fit is improving faster than the N number of adjusted EPR parameters, when a new species is included in the calculation. For the accepted equilibrium model including 7 species and 52 EPR parameters, the regression parameters R and R_n were found to be 0.99804 and 0.8981, respectively. Omitting one of the isomers of $CuH_{-2}L$, the regression parameters decreased considerably (45 EPR parameters, $R_n = 0.8619$). If Cu_2L_2 or $CuH_{-3}L$(b) was considered in addition to the accepted complexes the R_n parameter also decreased. On the other hand, assuming two isomers with the composition of $CuH_{-1}L$ both regression parameters increased (59 EPR parameters, $R = 0.99828$ and $R_n = 0.8985$). However, the increase of the R_n value is within the experimental error (0.04%), therefore the presence of a further isomer is not justified. Further details of the method and the evaluation procedure have been described previously.[45,46]

Determination of the superoxide dismutase activity

The SOD-like activity was studied at 298 K using the indirect method of Nitroblue Tetrazolium (NBT) reduction.[47] The superoxide anion was generated *in situ* by the xanthine/xanthine oxidase reaction, and detected spectrophotometrically by monitoring the reduction of NBT at 560 nm. The reactions were carried out in a phosphate buffer (5×10^{-2} M), containing NBT (5×10^{-5} M) and xanthine (1×10^{-4} M). The reaction was initiated by adding an appropriate amount of xanthine oxidase to generate $\Delta A_{560} = 0.025$–0.028 min^{-1}. The NBT reduction rate was measured in the presence and absence of the investigated system ($[Cu^{2+}]_{tot} = 0$–1×10^{-6} M). Control experiments, in the presence of Cu,Zn-SOD (0–5×10^{-8} M) were also carried out. In separate measurements, the activity of xanthine oxidase was monitored following urate production by spectrophotometry at 298 nm, to rule out any inhibition induced by the copper(II)–hhgh system. The SOD-like activity was then expressed by the IC_{50} values (concentration that causes 50% inhibition of NBT reduction).

Determination of the catecholase activity

The oxidation of 3,5-di-*tert*-butylcatechol (H_2dtbc) in the presence and absence of the copper(II)–hhgh system was monitored spectrophotometrically on a Unicam Helios α spectrophotometer at 298 K by following the increase of the 3,5-di-*tert*-butyl-*o*-benzoquinone absorption band at 400 nm ($\varepsilon = 1900$ M^{-1} cm^{-1}) in O_2-saturated 86 wt% methanol–water mixture. For the determination of the pH in this mixed solvent, the glass electrode was calibrated by standard aqueous buffer solutions (pH = 4.0, 7.0 and 10, Sigma) and then the actual pH was calculated by adding 0.28 units to the pH-meter reading, according to the method of Bates.[48] The ionization constants of water in 86 wt% methanol–water is $pK_w \sim 15.6$.[49] The auto-oxidation of 3,5-di-*tert*-butylcatechol was also determined for each substrate concentration and pH applied, and was then subtracted from the overall effect in order to obtain the extent of the oxidation reaction catalyzed by the copper(II)–hhgh complexes. The kinetic studies were carried out by the method of initial rates, but in some cases the integral method (up to 95% conversion) was also used. The reported data are the average of three parallel experiments. The maximum deviation from the main value did not exceed 10%.

Acknowledgements

This work was supported by the Hungarian Scientific Research Fund (OTKA T037385, T046953 and T043232) and by a Marie Curie Fellowship from the European Community program "Improving the Human Research Potential and the Socio-Economic Knowledge Base" (contract number "HPMF-CT-2002-01860"). T. G. thanks the János Bolyai Foundation for its support.

References

1 I. Sóvágó, in *Biocoordination Chemistry, ch.: Metal complexes of peptides and their derivatives*, ed. K. Burger, Ellis Horwood, Chichester, 1990.
2 H. Kozlowski, W. Bal, M. Dyba and T. Kowalik-Jankowska, *Coord. Chem. Rev.*, 1999, **184**, 319–346.
3 C. Harford and B. Sarkar, *Acc. Chem. Res.*, 1997, **30**, 123–130, and references therein.
4 E. C. Long, *Acc. Chem. Res.*, 1999, **32**, 827–836, and references therein.
5 E. Farkas, I. Sóvágó, T. Kiss and A. Gergely, *J. Chem. Soc., Dalton Trans.*, 1984, 611–614.
6 T. Gajda, B. Henry, A. Aubry and J.-J. Delpuech, *Inorg. Chem.*, 1996, **35**, 586–593.
7 J. H. Viles, E. Cohen, S. B. Prusiner, D. B. Goodin, P. E. Wright and H. J. Dyson, *Proc. Natl. Acad. Sci. USA*, 1999, **96**, 2042–2047.
8 E. Aronoff-Spencer, C. S. Burns, N. I. Avdievich, G. J. Gerfen, J. Peisach, W. E. Antholine, H. L. Ball, F. E. Cohen, S. B. Prusiner and G. L. Millhauser, *Biochemistry*, 2000, **39**, 13760–13771.
9 D. Valensin, F. M. Mancini, M. Luczkowski, A. Janicka, K. Wisniewska, E. Gaggelli, G. Valensin, L. Lankiewicz and H. Kozlowski, *Dalton Trans.*, 2004, 16–22.
10 S. Lehmann, *Curr. Opin. Chem. Biol.*, 2002, **6**, 187–192.
11 L. B. Corson, J. J. Strain, V. C. Culotta and D. W. Cleveland, *Proc. Natl. Acad. Sci. USA*, 1998, **95**, 6361–6366.
12 C. S. Burns, E. Aronoff-Spencer, C. M. Dunham, P. Lario, N. I. Avdievich, W. E. Antholine, M. M. Olmstead, A. Vrielink, G. J.

Gerfen, J. Peisach, W. G. Scott and G. L. Millhauser, *Biochemistry*, 2002, **41**, 3991–4001.
13 M. Orfei, M. C. Alcaro, G. Marcon, M. Chelli, M. Ginanneschi, H. Kozlowski, J. Brasun and L. Messori, *J. Inorg. Biochem.*, 2003, **97**, 299–307.
14 F. Fusetti, K. H. Schröter, R. A. Steiner, P. I. von Noort, T. Pijning, H. J. Rozeboom, K. H. Kalk, M. R. Egmond and B. W. Dijkstra, *Structure*, 2002, **10**, 259–268.
15 O. Spiga, M. Scarselli, A. Bernini, A. Ciutti, L. Giovannoni, F. Laschi, L. Bracci and N. Niccolai, *Biophys. Chem.*, 2002, **97**, 79–86.
16 W. Bal, J. Lukszo, K. Bialkowski and K. S. Kasprzak, *Chem. Res. Toxicol.*, 1998, **11**, 1014–1023.
17 R. P. Bonomo, L. Casella, L. De Gioia, H. Molinari, G. Impellizzeri, T. Jordan, G. Pappalardo, R. Purello and E. Rizzarelli, *J. Chem. Soc., Dalton Trans.*, 1997, 2387–2389.
18 P. Stanczak, M. Luczkowski, P. Juszczyk, Z. Grzonka and H. Kozlowski, *Dalton Trans.*, 2004, 2102–2107.
19 M. L. Pirosdos Santos, A. Faljoni-Aláro, A. S. Mangrich and A. M. da Costa Ferreira, *J. Inorg. Biochem.*, 1998, **71**, 71–78.
20 L. L. Constanzo, G. De Guidi, S. Giuffrida, E. Rizzarelli and G. Vecchio, *J. Inorg. Biochem.*, 1993, **50**, 273–281.
21 M. González-Arvarez, G. Alzuet, J. Borrás, L. del Castillo Agudo, J. M. Montejo-Bernardo and S. Garcia-Granda, *J. Biol. Inorg. Chem.*, 2003, **8**, 112–120.
22 B. Bóka, A. Myari, I. Sóvágó and N. Hadjiliadis, *J. Inorg. Biochem.*, 2004, **98**, 113–122.
23 R. P. Bonomo, V. Bruno, E. Conte, G. De Guido, D. La Mendola, G. Maccarone, F. Nicoletti, E. Rizzarelli, S. Sortino and G. Vecchio, *Dalton Trans.*, 2003, 4406–4415.
24 H. Ohtsu, Y. Shimazika, A. Odani, O. Yamauchi, W. Mori, S. Itoh and S. Fukuzumi, *J. Am. Chem. Soc.*, 2000, **122**, 5733–5741.
25 M. R. Malachowski, J. Carden, M. G. Davidson, W. L. Driessen and J. Reedijk, *Inorg. Chim. Acta*, 1997, **257**, 59–67.
26 J. Reim and B. Krebs, *J. Chem. Soc., Dalton Trans.*, 1997, 3793–3804.
27 P. Gentschev, N. Möller and B. Krebs, *Inorg. Chim. Acta*, 2000, **300–302**, 442–452.
28 C. Fernandes, A. Neves, A. J. Bortoluzzi, A. S. Mangrich, E. Rentschler, B. Szpoganicz and E. Schwingel, *Inorg. Chim. Acta*, 2001, **320**, 12–21.
29 J. Kaizer, J. Pap, G. Speier, L. Párkány, L. Korecz and A. Rockenbauer, *J. Inorg. Biochem.*, 2002, **91**, 190–198.
30 A. Neves, L. M. Rossi, A. J. Bortoluzzi, B. Szpoganicz, C. Wiezbicki, E. Schwingel, W. Haase and S. Ostrovsky, *Inorg. Chem.*, 2002, **41**, 1788–1794.
31 T. Gajda, B. Henry and J.-J. Delpuech, *Inorg. Chem.*, 1995, **34**, 2455–2460.
32 I. Török, T. Gajda, B. Gyurcsik, G. K. Tóth and A. Péter, *J. Chem. Soc., Dalton Trans.*, 1998, 1205–1212.
33 A. Jancsó, T. Gajda, E. Mulliez and L. Korecz, *J. Chem. Soc., Dalton Trans.*, 2000, 2679–2684.
34 A. Jancsó, I. Török, L. Korecz, A. Rockenbauer and T. Gajda, *J. Chem. Soc., Dalton Trans.*, 2002, 2601–2607.
35 D. Sanna, G. Micera, Cs. Kállay, V. Rigó and I. Sóvágó, *Dalton Trans.*, 2004, 2702–2707.
36 S. Bruni, F. Cariati, P. G. Daniele and E. Prenesti, *Spectrochim. Acta*, 2000, **56A**, 815–827.
37 E. Prenesti, P. G. Daniele, M. Prencipe and G. Ostacoli, *Polyhedron*, 1999, **18**, 3233–3241.
38 M. Casoralo, M. Chelli, M. Ginanneschi, F. Laschi, M. Muniz-Miranda, A. M. Papini and G. Sbrana, *Spectrochim. Acta*, 1999, **55A**, 1675–1689.
39 T. Klabunde, C. Eicken, J. C. Sacchettini and B. Krebs, *Nat. Struct. Biol.*, 1998, **5**, 1084–1090.
40 R. Griesser and H. Sigel, *Inorg. Chem.*, 1971, **10**, 2229–2232.
41 D. Chakraborty and P. K. Bhattacharya, *J. Chem. Soc., Dalton Trans.*, 1990, 3325–3327.
42 F. J. C. Rosotti and H. Rosotti, *The determination of stability constants*, McGraw-Hill Book Co., New York, 1962, p. 149.
43 E. Högfeldt, in *Stability Constants of Metal-Ion Complexes, Part A. Inorganic Ligands*, Pergamon, New York, 1982, p. 32.
44 L. Zékány, I. Nagypál, G. Peintler, *PSEQUAD for chemical equilibria, Technical Software Distributors*: Baltimore, MD, 1991.
45 A. Rockenbauer, T. Szabó-Plánka, Zs Árkosi and L. Korecz, *J. Am. Chem. Soc.*, 2001, **123**, 7646–7654.
46 T. Szabó-Plánka, A. Rockenbauer, L. Korecz and D. Nagy, *Polyhedron*, 2000, **19**, 1123–1131.
47 C. Beauchamp and I. Fridovich, *Anal. Biochem.*, 1974, **44**, 276–287.
48 R. G. Bates, *Determination of pH*, John Wiley & Sons, New York, 2nd edn, 1964, pp. 226-227.
49 C. H. Rochester, *J. Chem. Soc., Dalton Trans.*, 1972, 5–8.